Cellular/Molecular

Dendritic Generation of mGluR-Mediated Slow Afterdepolarization in Layer 5 Neurons of Prefrontal Cortex

Brian E. Kalmbach, Raymond A. Chitwood, Nikolai C. Dembrow, and Daniel Johnston
Center for Learning and Memory, University of Texas at Austin, Austin, Texas 78712

Many prefrontal cortex (PFC)-dependent tasks require individual neurons to fire persistently in response to brief stimuli. Persistent activity is proposed to involve changes in intrinsic properties, resulting in an increased sensitivity to inputs. The dendrite is particularly relevant to this hypothesis because it receives the majority of synaptic inputs and is enriched for conductances implicated in persistent firing. We provide evidence that dendritic conductances contribute to persistent activity-related changes in intrinsic properties. The effects of Group 1 metabotropic glutamate receptor (mGluR) activation on persistent activity-related properties were tested in two classes of rat L5 neurons with distinct membrane properties: those projecting to the pons (CPn) and those projecting across the commissure to the contralateral cortex (COM). mGluR activation produced long-term changes in the subthreshold properties of CPn, but not COM neurons. These changes were indicative of a decrease in hyperpolarization-activated cation nonselective current (I_h) at the soma and dendrite. mGluR activation also transiently increased the amplitude of the postburst slow afterdepolarization potential (sADP) at the soma of both neuron types. Interestingly, the sADP occurred along the extent of the apical dendrite in CPn and COM neurons. Simultaneous somatic/dendritic recordings revealed that the dendritic sADP does not result solely from passive propagation of the somatic sADP. Focal mGluR activation in L5, near the soma or at the border of L1/L2, near the tuft, generates a local sADP. This dendritic depolarization may act synergistically with synaptic input to regulate mnemonic activity in PFC.

Introduction

The prefrontal cortex (PFC) is involved in the temporal organization of information to guide future and ongoing behavior (Fuster, 2001). Consequently, the PFC is necessary for behaviors that rely on this ability, including working memory, decision-making, and goal-directed behavior (Goldman-Rakic, 1995; Miller, 2000; Rich and Shapiro, 2007, 2009). PFC involvement in these tasks appears to involve the ability of individual pyramidal neurons to fire persistently in response to transient stimuli (Funahashi et al., 1989; Jung et al., 1998; Pasupathy and Miller, 2005). Understanding the mechanisms of persistent activity is important for developing treatments for possible PFC-related disorders (e.g., see Egan and Weinberger, 1997; Bremner et al., 1999; Courchesne and Pierce, 2005; Fineberg et al., 2009; Goldstein and Volkow, 2011).

Persistent activity is thought to involve changes in the input/output properties of pyramidal neurons by at least two nonmutually exclusive mechanisms. The first involves the postburst afterdepolarization (sADP) and can result in the transformation of transient input into self-sustained persistent activity (Schwindt et al., 1988; Haj-Dahmane and Andrade, 1998; Hasselmo and Stern, 2006; Sidiropoulou et al., 2009). In the second, the integrative properties of the cell are enhanced through downregulation of the hyperpolarization-activated cation nonselective current (I_h; Wang et al., 2007). The dendrite is particularly relevant to both mechanisms because it is where the bulk of inputs arrive and is enriched for I_h (Williams and Stuart, 2000).

Assessing these putative persistent activity mechanisms is complicated by evidence that the physiological properties of L5 neurons depend on their long-range projection targets (Christophe, 2005; Molnár and Cheung, 2006; Hattox and Nelson, 2007; Otsuka and Kawaguchi, 2008; Dembrow et al., 2010; Sheets et al., 2011; Avesar and Gulledge, 2012). In the medial PFC (mPFC), we have identified two classes of L5 neurons with distinct membrane properties (Dembrow et al., 2010). Neurons projecting subcortically to the pons (CPn) have membrane properties that endow them with I_h-dependent resonance, whereas neurons projecting across the commissure (COM) are nonresonant. Furthermore, neurotransmitter systems have distinct effects on these projection classes, highlighting the general possibility that the effect of neuromodulation depends on the projection type.

We tested the effects of metabotropic glutamate receptor (mGluR) activation, which has been reported to modulate the sADP and subthreshold membrane properties (Greene et al., 1994; Brager and Johnston, 2007; Sidiropoulou et al., 2009), on the somatic and dendritic properties of both classes of neurons. We find that mGluR activation causes long-term changes in subthreshold membrane properties exclusively in CPn neurons. These subthreshold changes occur in the dendrite and soma and

Received May 13, 2013; revised July 13, 2013; accepted July 16, 2013.

Author contributions: B.E.K., R.A.C., N.C.D., and D.J. designed research; B.E.K., R.A.C., and N.C.D. performed research; B.E.K., R.A.C., and N.C.D. analyzed data; B.E.K., R.A.C., N.C.D., and D.J. wrote the paper.

This work was supported by National Institutes of Health Grant R01 MH094839 to D.J. and Grant F32 MH090694 to B.E.K., a McKnight Foundation Grant to D.J., and a NARSAD Young Investigator Award to N.D. We thank Eedann McCord for assistance with surgery.

The authors declare no competing financial interests.

Correspondence should be addressed to Dr. Brian E. Kalmbach, Center for Learning and Memory, University of Texas at Austin, 1 University Station, C7000, Austin, TX 78712. E-mail: brian@mail.clm.utexas.edu.

DOI:10.1523/JNEUROSCI.2018-13.2013

 0270-6474/13/3313518-15$15.00/0

are consistent with a decrease in I_h. We also observe an sADP along the extent of the apical dendrite (from the soma to the start of the tuft) in both neuron types. This sADP can be generated locally in the soma or dendrite and may act synergistically with changes in passive properties to influence mnemonic processes.

Materials and Methods

Bead infusions. All procedures involving animals were approved by the University of Texas at Austin Institutional Animal Care and Use Committee. Male Sprague Dawley rats 8–14 weeks old were anesthetized with isoflurane (1–4% mixed in oxygen) and prepared for stereotaxic injection of red retrograde transported fluorescent-labeled microspheres (Lumafluor). Beads were injected into the pons (left or right; 7.4 mm posterior, 1.1 mm lateral, 9.8 mm ventral to bregma) or mPFC (left or right; 2 injections: 2.5–3.5 mm anterior, 0.8 mm lateral, and 4–4.4 mm ventral to bregma) using a glass pipette (10–15 μm diameter tip) connected to a Nanoject II auto-nanoliter injector (Drummond Scientific) at a rate of 23 nl/s. Pons injections consisted of three 50.6 nl injections at the same location delivered every 10 s. mPFC injections consisted of two 50.6 nl injections at two different locations separated by 5 min. For all injections, the pipette was left in place for 5 min before removing it from the brain. Rats were given analgesics (carprofen; 5 mg/kg) and recovered for at least 2 d before their use in physiological experiments.

Slice preparation. Male Sprague Dawley rats 8–15 weeks old were anesthetized with a ketamine (100 mg/kg)/xylazine (10 mg/kg) mixture and were perfused through the heart with ice-cold saline consisting of the following (in mM): 2.5 KCl, 1.25 NaH_2PO_4, 25 $NaHCO_3$, 0.5 $CaCl_2$, 7 $MgCl_2$, 7 dextrose, 205 sucrose, 1.3 ascorbate, and 3 sodium pyruvate (bubbled with 95% O_2/5% CO_2 to maintain pH at ~7.4). Brains were removed, and a blocking cut was made ~3 mm posterior to bregma at an angle of ~11° off coronal to maintain the plane of the dendrites within the slice. A vibrating tissue slicer (Vibratome 3000, Vibratome) was used to make 300-μm-thick coronal sections. Slices were cut in ice-cold saline that was identical to the saline used during the perfusion. Slices were subsequently held for 30 min at 35°C in a chamber filled with artificial CSF (aCSF) consisting of (in mM) as follows: 125 NaCl, 2.5 KCl, 1.25 NaH_2PO_4, 25 $NaHCO_3$, 2 $CaCl_2$, 2 $MgCl_2$, 10–12.5 dextrose, and 3 sodium pyruvate (bubbled with 95% O_2/5% CO_2) and then at room temperature until the time of recording.

Whole-cell recordings. Recordings were made from L5 pyramidal neurons in the anterior cingulate or prelimbic regions of mPFC. Slices were placed in a submerged, heated (32–34°C) recording chamber that was continually perfused (1–2 ml/min) with bubbled aCSF identical to the holding aCSF, except that it contained slightly more KCl (3 mM) and less $MgCl_2$ (1 mM; the holding aCSF contained different concentrations of these compounds to decrease the possibility of spontaneous activity/plasticity). With the exception of a few simultaneous soma and dendrite whole-cell recordings, the following receptor antagonists were added to the recording aCSF (in μM) as follows: 50 D,L-APV, or 25 D-APV, 20 DNQX, 5 CGP, 2 gabazine, and 1 atropine. Slices were viewed with either a Zeiss Axioskop using differential interference contrast optics or a two-photon laser-scanning microscope (Leica SP5 RS) using Dodt contrast. Bead-labeled neurons or Alexa-594-filled neurons were visualized using either two-photon excitation at 840 nm or through the use of a mercury lamp and a 540 nm/605 nm excitation/emission filter set. Simultaneous soma and dendrite recordings were made by first patching the soma of a L5 neuron with a pipette containing Alexa-594 (40 μM). This permitted the dendrite to be visualized and subsequently patched with a second pipette using simultaneous Dodt contrast and fluorescence microscopy. Patch pipettes (4–8 MΩ) were pulled from borosilicate glass and filled with an internal recording solution consisting of (in mM) as follows: 120 K gluconate, 16 KCl, 10 HEPES, 8 NaCl, 7 K_2 phosphocreatine, 0.3 Na-GTP, and 4 Mg-ATP (pH 7.3 with KOH). For a subset of experiments, K gluconate was replaced with 120 mM K methylsulfate. Neurobiotin (Vector Laboratories; 0.1–0.2%) was also included for histological processing. For all experiments involving dendritic recordings and some experiments involving somatic recordings, Alexa-594 (15–40 μM; Invitrogen) was also included in the internal recording solution to determine the recording location. Alexa-filled neurons were visualized only upon termination of the recording when excited with a mercury lamp or with low laser power when excited with 2-photon microscopy. For experiments in which 20 mM 4K-BAPTA was included in the recording pipette, the concentration of Kgluconate was reduced to 40 and 60 mM sucrose was added to maintain osmotic balance.

Data were acquired using a Dagan BVC-700 (Dagan) amplifier and custom data acquisition software written using Igor Pro (Wavemetrics) or a Multiclamp 700B (Molecular Devices) amplifier and AxoGraph X (AxoGraph Scientific) data acquisition software. Data were acquired at 10–50 kHz, filtered at 5–10 kHz, and digitized by an ITC-18 (InstruTech) interface. Pipette capacitance was compensated, and the bridge was balanced before each recording. Series resistance was monitored throughout each experiment and was 10–25 MΩ for somatic recordings and 13–40 MΩ for dendritic recordings. Voltages are not corrected for the liquid-junction potential (estimated as ~12 mV based on relative ionic mobilities and charge).

Pressure application of DHPG. Focal application (puffing) of 200 μM R,S-DHPG was accomplished with a large diameter glass pipette (10–15 μm) positioned ~20 μm above the slice directly over the soma or at the beginning of the tuft of the recorded neuron. DHPG was dissolved in the standard recording aCSF and 100 μM Fast Green (Fisher) was added to monitor the spread of the puffing solution. Low pressure, 1 s puffs spread ~150 μm in the axis of the main apical dendrite and caused little tissue movement. Puffing the recording aCSF alone during somatic ($n = 3$) or dendritic ($n = 3$, range 315–495, mean 377 ± 59 μm from soma) whole-cell recordings did not significantly affect the sADP (Δ sADP postpuff, dendrite = −0.02 ± 0.15 mV; soma = 0.12 ± 0.05 mV). To examine the stability of the sADP, we applied 1 s puffs of DHPG to the soma every 90 s upon break-in while recording at the soma. There was no difference in the peak amplitude of the first versus last sADP ($n = 4$, first = 3.6 ± 0.98 mV, last 3.5 ± 1.2 mV, $p = 0.94$, paired t test).

Data analysis. Data were analyzed using either custom analysis software written in Igor Pro or using AxoGraph X. Input resistance (R_N) was calculated from the linear portion of the current–voltage relationship generated in response to a family of 1000 ms current injections (−150 to +50 pA, 20 pA steps). The maximum and steady-state voltage deflections were used to determine the maximum and steady-state R_N, respectively. Voltage sag and rebound slope were also calculated from the voltage response to this same family of current injections. Voltage sag was defined as the ratio of maximum to steady-state R_N. Rebound slope was calculated from the slope of the rebound amplitude as a function of steady-state membrane potential. The functional membrane time constant was defined as the slow component of a double-exponential fit of the average voltage decay in response to alternating depolarizing and hyperpolarizing current injections (200–400 pA, 1–2 ms). Resonance was determined from the voltage response to a constant amplitude sinusoidal current injection that linearly increased in frequency from 1 to 15 Hz in 15 s. The impedance amplitude profile (ZAP) was constructed from the ratio of the fast Fourier transform of the voltage response to the fast Fourier transform of the current injection. The peak of the ZAP was defined as the resonant frequency. Input-output plots were constructed by plotting the number of spikes in response to a family of 750 ms current injections (50–350 pA, 20 pA steps). The peak and integral of the slow after-hyperpolarization (AHP) and sADP were measured in response to trains of 5, 1, or 2 ms current injections (1.5–3 nA). Each spike protocol was administered three times. If persistent activity was observed following any of these protocols, the neuron was considered to have fired persistently. The sADP was defined as the difference in the average membrane potential 50 ms before the onset of the stimulus and the peak voltage deflection after the burst of spikes. The sADP during baseline conditions was measured at the same time point as the peak sADP during DHPG application. The AHP was defined as the minimum voltage after the spike train. The passive propagation of slow ADP-like events from the soma to dendrite was calculated by injecting a double-exponential current waveform through the somatic electrode and measuring the voltage response at the soma and dendrite. The rise time of the current injection was adjusted to approximate the kinetics of the sADP for each cell.

For recordings from nonlabeled neurons, the presence or absence of resonance was used to classify neurons into projection types. Based on previous observations (Dembrow et al., 2010), neurons were classified as CPn-type if they displayed membrane resonance (>2.2 Hz), whereas neurons were classified as COM-type if they did not (<2.2 Hz). Labeled neurons are referred to as CPn and COM, whereas unlabeled or mixed datasets are referred to as CPn-type and COM-type. This classification scheme is especially relevant for dendritic recordings, where the presence of Alexa-594 in the recording pipette made it difficult to identify the presence of Lumafluor beads at the soma.

Repeated-measures ANOVA (RM-ANOVA), mixed-factors ANOVA, and *post hoc t* tests were used to test for statistical differences between experimental conditions. Bonferonni correction was used to correct for multiple comparisons. Pearson's product moment correlation was used to test for statistically significant correlations between variables. Error bars represent SEM. Statistical analyses were performed in Igor or Excel. Data are presented as mean ± SEM.

Drugs. All drugs were prepared from concentrated stock solutions in water (gabazine, atropine, DNQX, ZD7288, R,S-DHPG, D-APV), equivalent NaOH (D, L-APV; LY367385) or DMSO (MPEP, CGP55845; final concentration of DMSO ≤ 0.1%) as appropriate. DHPG stocks were made fresh weekly. All drugs were obtained from Ascent scientific/Abcam Pharmaceutical.

Results

mGluR-mediated slow afterdepolarization in CPn and COM neurons

Electrogenesis, in the form of a slowly developing after depolarization (sADP) after bursts of action potentials, is implicated in persistent firing (Schwindt et al., 1988; Haj-Dahmane and Andrade, 1996, 1998; Egorov et al., 2002; Hasselmo and Stern, 2006; Hagenston et al., 2007; Yoshida et al., 2008; Sidiropoulou et al., 2009; Dembrow et al., 2010; Gee et al., 2012). Muscarinic acetylcholine receptor (mAChR) activation induces an sADP that is larger in CPn compared with COM neurons. Furthermore, CPn neurons are more likely to fire persistently than COM neurons upon cholinergic modulation (Dembrow et al., 2010). Because Group 1 mGluRs and mAChRs are both G_q protein-coupled receptors that activate similar signaling cascades (Anwyl, 1999; Krause et al., 2002), we tested whether mGluR activation (1) induces a larger sADP in CPn compared with COM neurons and (2) produces persistent activity in CPn neurons more often than COM neurons. To test these hypotheses, we injected trains of brief depolarizing current pulses at the soma of both neuron types to elicit either single or bursts of 5 action potentials (20 and 50 Hz) from a membrane potential of −60 mV before and after a 10 min bath application of the Group 1 mGluR agonist, DHPG (20 μM; Fig. 1). In a subset of experiments, the 10 min bath application was followed by a 30 min washout to test for long-term effects.

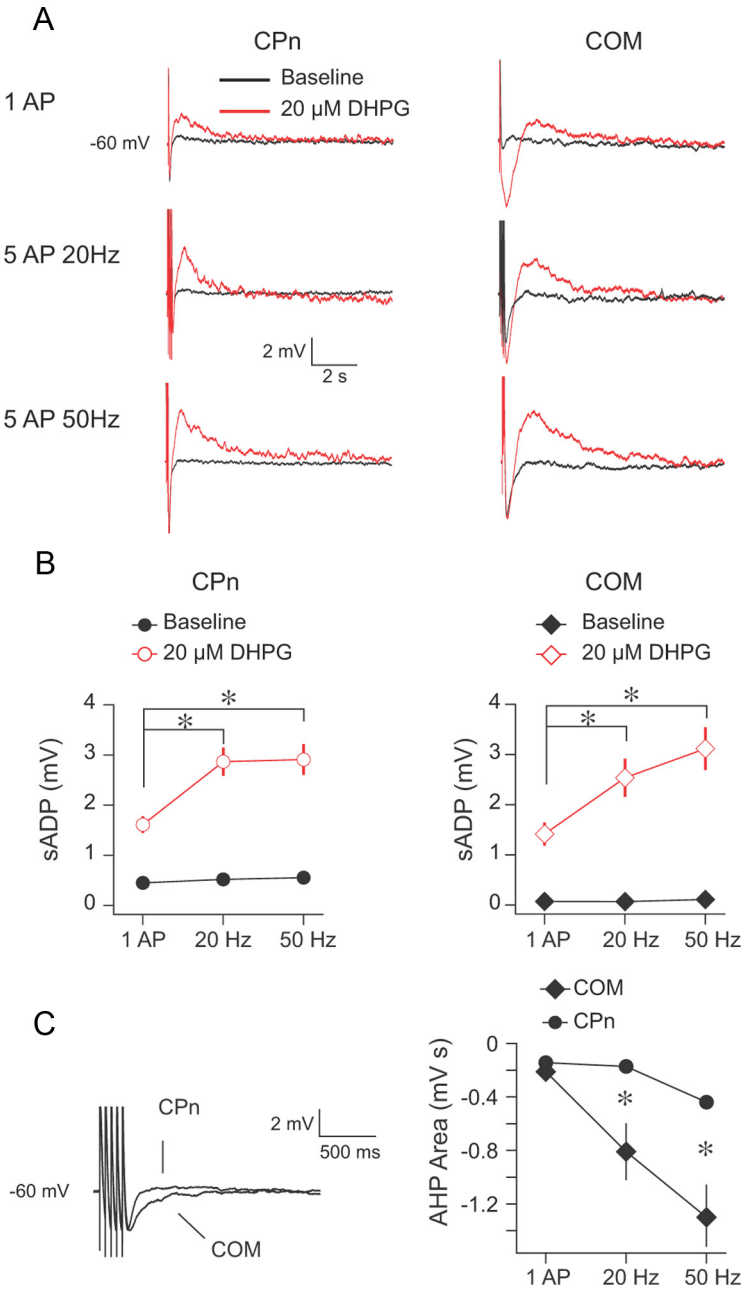

Figure 1. Group 1 mGluR activation produces an sADP in CPn and COM neurons. ***A***, CPn and COM neurons were driven to fire single or bursts of action potentials from a common membrane potential (−60 mV) before and after a 10 min application of 20 μM DHPG. ***B***, In both CPn ($n = 12$) and COM ($n = 10$) neurons, the amplitude of the sADP increased after DHPG application (CPn, $p < 0.001$, RM-ANOVA; COM, $p < 0.001$, RM-ANOVA). For both cell types, the burst protocols produced a larger sADP than a single action potential. *$p < 0.001$ (*post hoc* comparisons). The effect of DHPG on the sADP was not statistically different in CPn versus COM neurons ($p = 0.1$, mixed ANOVA). The sADP during baseline conditions was measured at the same time point as the peak of the sADP during DHPG application. ***C***, The area of the AHP was larger in COM neurons compared with CPn neurons during baseline conditions ($p < 0.001$, mixed ANOVA). *$p < 0.01$ (*post hoc* comparisons).

In contrast to mAChR activation, the effect of mGluR activation on the sADP was similar in CPn and COM neurons (Fig. 1). In both CPn ($n = 12$) and COM ($n = 10$) neurons, the peak sADP amplitude was dependent on the number/frequency of action potentials (CPn and COM, $p < 0.001$; RM-ANOVAs) with both burst protocols producing a larger sADP than a single action potential (Fig. 1*A*,*B*; CPn and COM, $p < 0.01$; *post hoc* compar-

isons). There was no statistical difference in the amplitude of the sADP in CPn compared with COM neurons ($p = 0.1$; mixed ANOVA). The effects of DHPG on the sADP were short-term in that they fully reversed after 30 min of washout in both neuron types (data not shown; CPn, $n = 4$, $\Delta = 0.22 \pm 0.36$; $p = 0.56$; COM, $n = 4$, $\Delta = -0.03 \pm 0.05$, $p = 0.30$; baseline vs post 30 min washout, RM-ANOVA). The same pattern of results was observed for the integral of the sADP (data not shown). We observed persistent activity in CPn neurons, albeit rarely (5 of 12 neurons), but more often than in COM neurons (1 of 10 neurons) upon mGluR activation (see Fig. 4). Finally, we observed an sADP (50 Hz, CPn = 1.52 ± 0.14 mV, $n = 3$; COM = 2.13 ± 0.54, $n = 3$) and persistent activity (CPn = 1 of 3; COM = 1 of 3) after the application of DHPG in both neuron types with a K methylsulfate based internal.

Group 1 mGluR activation has also been reported to modulate K^+ currents that mediate the AHPs that follow bursts of action potentials on the scale of tens to thousands of milliseconds (Greene et al., 1994; Mannaioni et al., 2001; Sourdet et al., 2003; Young et al., 2004; Hagenston et al., 2007). We thus also tested for differences in the effects of DHPG on the AHP in CPn versus COM neurons. Under baseline conditions, CPn and COM neurons displayed an AHP that was dependent on the number/frequency of action potentials (Fig. 1*C*; CPn and COM $p < 0.002$; RM-ANOVA). Although there was no difference in the peak amplitude of the AHP in CPn compared with COM neurons (data not shown; 1 AP, CPn = −2.06 ± 0.31, COM = −1.62 ± 0.45; 20 Hz, CPn = −2.62 ± 0.16, COM = −3.22 ± 0.49; 50 Hz, CPn = −5.31 ± 0.32, COM = −4.38 ± 0.66; $p = 0.54$; mixed ANOVA), the integral was larger in COM neurons compared with CPn neurons for both burst protocols (Fig. 1*C*; $p < 0.01$; *post hoc* comparisons). This difference was more apparent with a K methylsulfate-based internal (e.g., 50 Hz, CPn = −1981.52 ± 257.93 mV s, $n = 7$; COM = −10,791.36 ± 1385.77 mV s, $n = 5$; $p < 0.001$, independent samples *t* test). Although 20 μM DHPG clearly affected the AHP of both neuron types in some instances, this effect was highly variable, increasing the AHP in some cases (e.g., COM neuron in Fig. 1*A*) and decreasing it in others (Δ post DHPG; COM; 1 AP, −0.82 ± 0.58; 20 Hz, −0.65 ± 0.34; 50 Hz, 0.33 ± 0.31; all $p > 0.31$; CPn; 1 AP, 0.6 ± 0.28; 20 Hz, 0.57 ± 0.29; 50 Hz, 0.72 ± 0.46; all $p > 0.09$; RM-ANOVAs).

mGluR-mediated modulation of subthreshold membrane properties in CPn versus COM neurons

Persistent activity has also been proposed to involve a decrease in I_h that results in the strengthening of PFC networks (Wang et al., 2007). To test whether mGluR activation produces changes in I_h, we compared several I_h-sensitive physiological measurements (Hutcheon et al., 1996; Hutcheon and Yarom, 2000; Hu et al., 2002; Poolos et al., 2002; Robinson and Siegelbaum, 2003; Nolan et al., 2004; Brager and Johnston, 2007; Narayanan and Johnston, 2007, 2008) (R_N, voltage sag, rebound potential, and resonance) before and 30 min after a 10 min bath application of 20 μM DHPG in both neuron types. In CPn neurons ($n = 11$), DHPG produced an increase in R_N within the first 10 min of application ($p < 0.001$; *post hoc* comparison vs baseline) that persisted through washout ($p < 0.001$; *post hoc* comparison vs baseline; Fig. 2*A–C*). There was also a decrease in sag, rebound, and resonance after washout (Fig. 2*B–E*; $p < 0.001$; paired *t* tests). In contrast, in COM neurons ($n = 9$), there was no significant change in R_N within the first 10 min of DHPG application or after washout (both $p > 0.05$; *post hoc* comparisons vs baseline; Fig. 2*A–C*). Furthermore, there were no changes in sag, rebound, or resonance (Fig. 2*B–E*; $p > 0.05$, paired *t* tests). In a subset of experiments, we monitored resting membrane potential (RMP) throughout the 10 min DHPG application and 30 min washout. In CPn neurons, DHPG produced a hyperpolarization of the RMP that persisted through 30 min of washout (Fig. 2*A*,*F*; $n = 7$, $p < 0.001$, baseline vs peak change; $p = 0.03$, baseline vs post 30 min; *post hoc* comparisons). In contrast, DHPG produced a depolarization of the RMP in COM neurons that was reversed by 30 min of washout (Fig. 2*A*,*F*; $n = 4$, $p = 0.009$, baseline vs peak change; $p = 0.71$ baseline vs post 30 min; *post hoc* comparisons). Together, these data suggest that Group 1 mGluR activation results in a long-lasting decrease in I_h in CPn, but not COM neurons.

We next tested whether the apparent decrease in I_h in CPn neurons affects action potential generation in response to depolarizing current injections, as has been reported in other neuron types (Brager and Johnston, 2007). We measured the number of action potentials evoked by a family of depolarizing current injections from a common membrane potential (−65 mV) in both CPn ($n = 9$) and COM ($n = 9$) neurons before and 30 min after the 10 min application of 20 μM DHPG (Fig. 3). DHPG produced a statistically significant increase in the number of action potentials evoked by a given current injection in CPn ($p < 0.001$, RM-ANOVA) but not COM neurons ($p = 0.11$, RM-ANOVA; Fig. 3*A*). However, there was no increase in spike generation after DHPG application in CPn neurons when measurements were made from RMP ($n = 7$, $p = 0.25$, RM-ANOVA; Fig. 3*B*). This suggests that, in terms of spike generation, the increased R_N observed upon DHPG application in CPn neurons is offset by hyperpolarization of the RMP. Furthermore, because measurements were made 30 min after the end of the application of DHPG, the increase in spike generation observed at −65 mV is unlikely attributable to conductances involved in the sADP.

Finally, we provided additional, pharmacological evidence that (1) the short- and long-term changes we observed are mediated by Group 1 mGluRs and (2) the long-term changes we observed in CPn neurons involve changes in I_h. In the continued presence of the mGluR 5 blocker MPEP (40 μM) and the mGluR1 blocker LY367385 (50 μM), DHPG did not produce significant changes in the subthreshold properties of CPn neurons (Fig. 4*A*; $p > 0.1$, paired *t* tests). MPEP and LY367385 also blocked the DHPG-induced increase in the sADP in CPn (50 Hz; DHPG, 2.90 ± 0.31 mV; DHPG and LY367385 + MPEP, 0.75 ± 0.11 mV, $p < 0.001$ independent samples *t* test) and COM neurons (50 Hz; DHPG, 3.12 ± 0.43 mV; DHPG and LY367385 + MPEP, 1.02 ± 0.17 mV, $p < 0.001$ independent samples *t* test; Fig. 4*B*). Furthermore, when the Ca^{2+} chelator BAPTA (20 mM) was included in the recording pipette, DHPG failed to produce significant changes in the subthreshold properties of CPn neurons (Fig. 4*A*; all $p > 0.1$, paired *t* tests). DHPG also failed to produce changes in the subthreshold properties of CPn neurons when the HCN channel (the channel that conducts I_h) blocker ZD7288 (10 μM) was included in the recording pipette (Fig. 4*A*; all $p > 0.25$, paired *t* tests). Interestingly, applying DHPG in the presence of ZD7288 produced a larger sADP in both cell types compared with DHPG alone (CPn, $p = 0.001$; COM, $p = 0.02$, paired *t* tests; Fig. 4*B*). With ZD7288 present, we also observed more persistent firing after DHPG application compared with DHPG alone, perhaps because of the larger amplitude of the sADP (Fig. 4*C*).

Together, these data suggest that Group 1 mGluR activation produces changes in L5 mPFC pyramidal neurons consistent with two putative mechanisms of persistent activity. mGluR activation produces long-lasting changes in the sub-

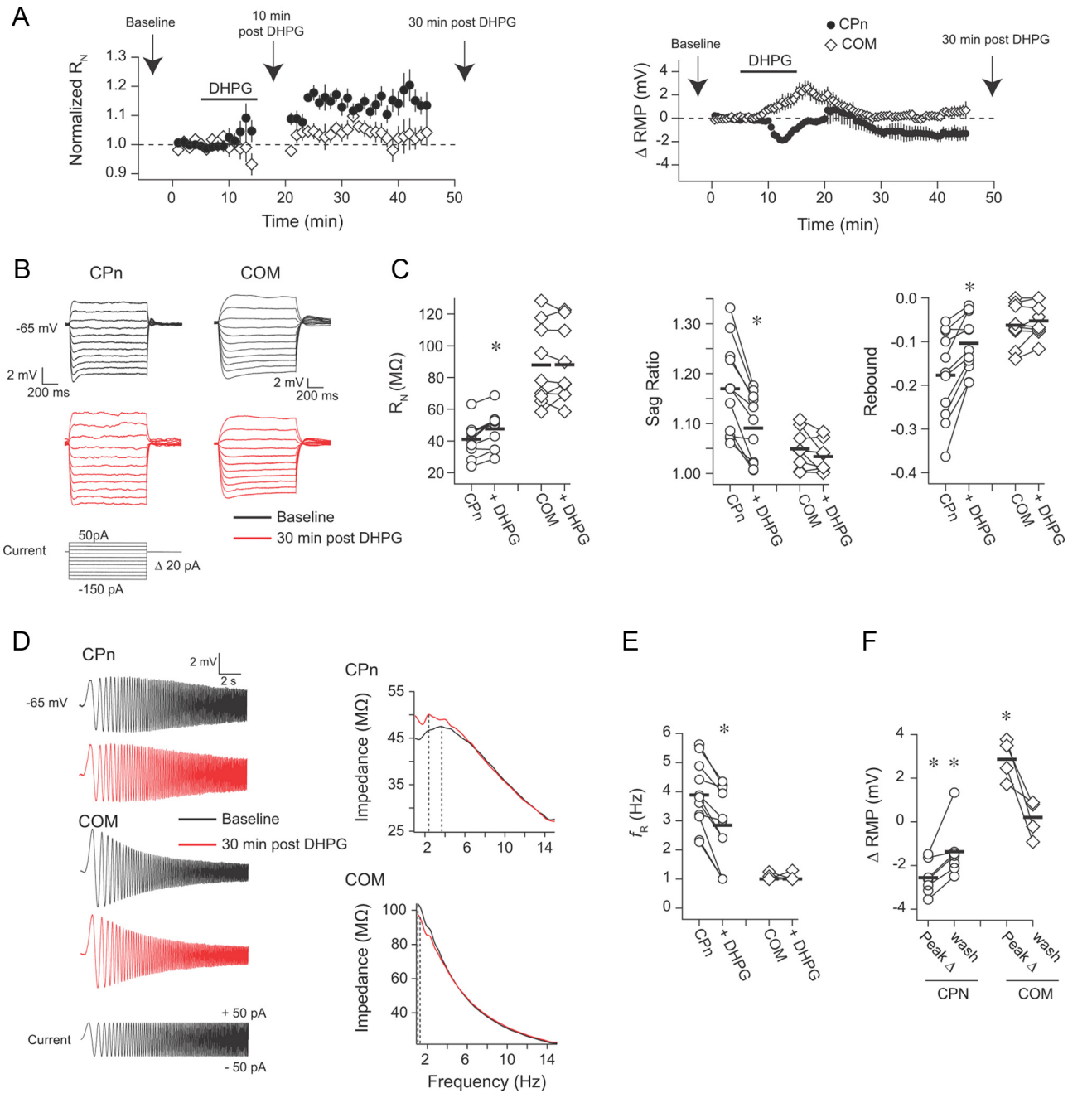

Figure 2. Group 1 mGluR activation produces long-lasting changes in the subthreshold membrane properties of CPn but not COM neurons. ***A***, RMP or R_N at −65 mV was monitored over time in CPn and COM neurons. The application of DHPG produced a long-term hyperpolarization of RMP and an increase in R_N in CPn neurons. In contrast, in COM neurons, there was only a transient depolarization of RMP. Arrows indicate the relevant times at which measurements were made for subsequent panels. The sADP was measured during the 10 min post-DHPG time point. ***B***, Sample voltage responses to a family of current injections before and 30 min after a 10 min application of DHPG. R_N, sag, and rebound were calculated from these voltage responses. ***C***, DHPG produced an increase in R_N and a decrease in sag and rebound in CPn neurons. There were no changes in these measurements in COM neurons. $^*p < 0.001$ (paired *t* test). ***D***, Sample voltage responses to a chirp stimulus current injection. These responses were used to create the impedance amplitude profiles (ZAPs) shown at the right. The peak of the ZAP is the resonant frequency. ***E***, DHPG produced a decrease in resonance in CPn neurons, whereas resonance in COM neurons remained 1 Hz. All I_h-related measurements were made at −65 mV. $^*p < 0.001$ (paired *t* test). ***F***, DHPG produced a long-lasting hyperpolarization of the RMP in CPn neurons and a transient depolarization of the RMP in COM neurons. The peak change refers to the peak change in RMP at any time during the DHPG application and washout. $^*p < 0.05$ (*post hoc* comparisons to baseline RMP).

threshold membrane properties of CPn neurons and transient changes in the sADP of CPn and COM neurons. The long-lasting changes in CPn neurons are consistent with a decrease in I_h and require a rise in intracellular Ca^{2+}. Finally, I_h appears to affect the size of the sADP and the propensity to fire persistently in both neuron types.

Projection-specific dendritic membrane properties

HCN channel expression in cerebral cortex increases with distance from the soma (Williams and Stuart, 2000; Berger et al., 2001; Lörincz et al., 2002; Atkinson and Williams, 2009; Breton and Stuart, 2009), making the apical dendritic compartment a prime candidate for the modulation of I_h. mGluR activation has

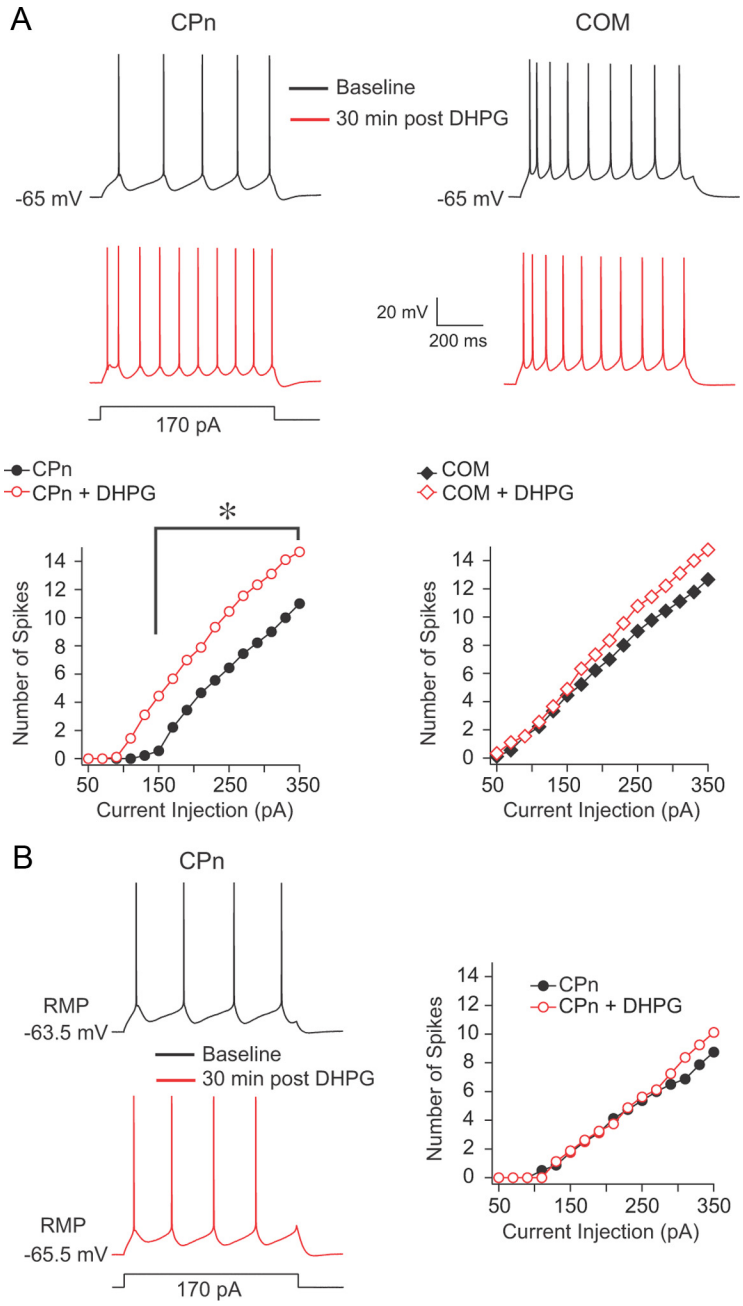

Figure 3. Effect of Group 1 mGluR activation on action potential generation in L5 prefrontal neurons. ***A***, CPn and COM neurons were driven to fire action potentials in response to a series of depolarizing current injections (50–350 pA, 20 pA steps) from a common membrane potential (−65 mV) before and 30 min after a 10 min DHPG application. DHPG produced a statistically significant increase in the number of spikes to a given current injection in CPn ($p < 0.001$, RM-ANOVA), but not COM neurons ($p = 0.11$, RM-ANOVA *$p < 0.003$ (*post hoc* comparisons). ***B***, Same experimental design as in ***A***, except that cells were driven to fire action potentials from their RMP ($p = 0.25$, RM-ANOVA).

been reported to produce Ca^{2+} waves in the apical dendrite of L5 pyramidal neurons (Larkum et al., 2003; Hagenston et al., 2007). These waves are associated with the sADP at the soma, leaving open the possibility that the sADP has a dendritic component. For these reasons, we asked whether there is a dendritic contribution to the mGluR-mediated short- and long-term changes we observed at the soma.

The intrinsic membrane properties of L5 dendrites have been reported previously (Berger et al., 2001). However, heterogeneity in these properties depending on the projection target remains unexplored. Thus, before testing the effects of mGluR activation, we first tested whether the distinct membrane properties of CPn versus COM neurons observed at the soma (Christophe, 2005; Otsuka and Kawaguchi, 2008; Dembrow et al., 2010; Sheets et al., 2011; Avesar and Gulledge, 2012) extend to the dendritic compartment. Because the fluorescent marker we used to label CPn and COM neurons is restricted to the soma, we patched L5 dendrites at various distances from the soma, blind to the projection target of the cell (Fig. 5*A*). Inclusion of Alexa-594 in the recording pipette permitted us to trace the dendrite back to the L5 soma upon termination of the recording. Recordings revealed two populations of L5 dendrites: (1) those with membrane properties similar to CPn neurons at the soma (CPn-type; $n = 43$) and (2) those with membrane properties similar to COM neurons at the soma (COM-type; $n = 28$). At RMP, CPn-type dendrites displayed a distance-dependent decrease in R_N ($r^2 = 0.22$, $p = 0.001$) and an increase in rebound ($r^2 = 0.53$, $p < 0.001$), membrane resonance ($r^2 = 0.53$, $p < 0.001$; Fig. 5*B*,*C*), and sag ($r^2 = 0.53$, $p < 0.001$; data not shown). RMP also became more depolarized with distance from the soma ($r^2 = 0.53$, $p < 0.001$; data not shown). In contrast, in the COM-type dendrite R_N ($r^2 = 0.07$, $p = 0.18$), rebound ($r^2 = 0.07$, $p = 0.18$), resonance ($r^2 = 0.10$, $p = 0.10$; Fig. 5*B*,*C*), sag ($r^2 = 0.12$, $p = 0.07$; data not shown), and RMP ($r^2 = 0.01$, $p = 0.90$; data not shown) were not distance dependent. However, we cannot rule out the possibility that there are subtle distance-dependent differences in these measurements within single neurons (see, e.g., simultaneous soma/dendrite recordings in the subsequent paragraph).

To confirm that these two populations of dendrites belong to CPn and COM neurons, we compared the subthreshold membrane properties of the dendrite to the soma in both neuron types using simultaneous somatic/dendritic whole-cell recordings (Fig. 6*A*). In CPn-type neurons (Fig. 6*B*,*C*; $n = 15$, range = 130–550 μm, mean = 359 ± 35 μm distance between recording locations), R_N at the dendrite was significantly lower than at the soma and the dendrite had more rebound, resonance, and sag (sag not shown; soma 1.15 ± 0.02, dendrite 1.33 ± 0.05; all $p < 0.02$, paired t tests) compared with the soma. In contrast, in COM neurons (Fig. 6*B*,*C*; $n = 12$, range = 80–450 μm, mean = 241 ± 34 μm distance between recording locations), there was slightly more rebound in the dendrite compared with the soma ($p = 0.005$, paired t test), but no difference in sag (soma 1.02 ± 0.01, dendrite 1.03 ± 0.01; data not shown), R_N, or resonance (all $p > 0.40$; paired t tests). RMP was more depolarized in the dendrite compared with the soma in both neuron types (CPn, soma −65.99 ±

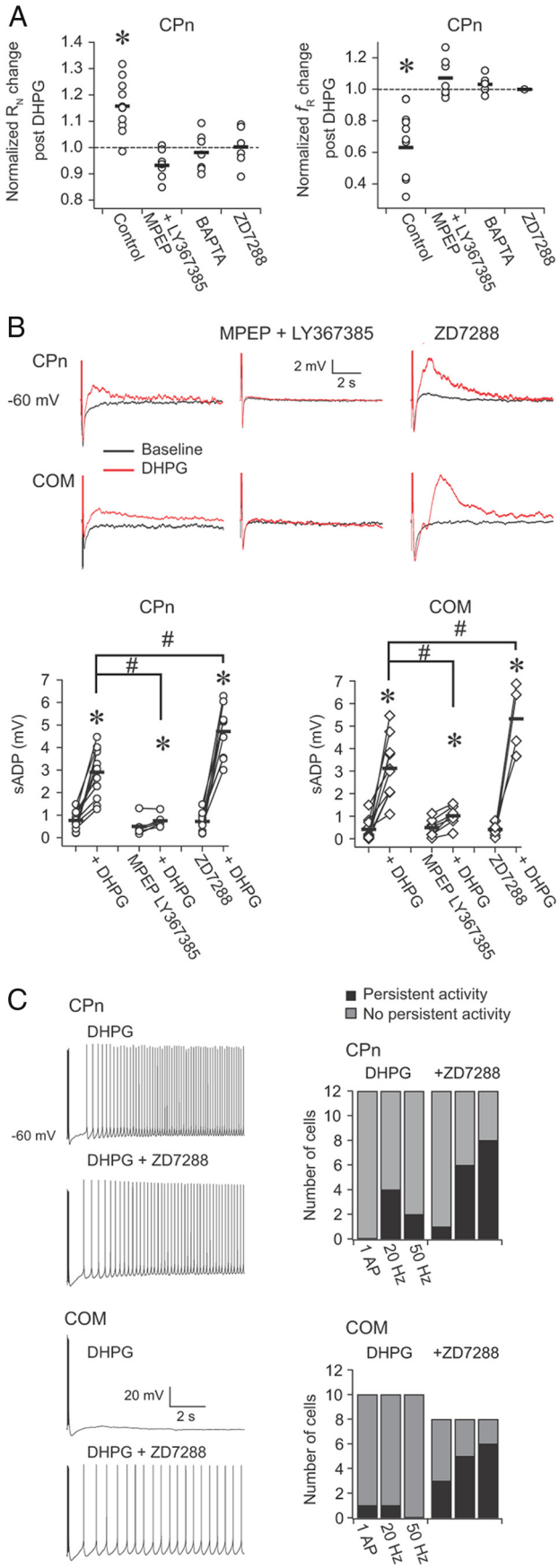

Figure 4. Mechanisms contributing to short- and long-term changes in L5 neurons after DHPG application. ***A***, There were no changes in the subthreshold membrane properties of CPn neurons in response to 20 μM DHPG in the continued presence of the mGluR5 antagonist MPEP (40 μM) and the mGluR1 antagonist LY367385 (50 μM). There were also no changes when 20 mM BAPTA or 10 μM ZD7288 was included in the recording pipette. Similar results were obtained for sag and rebound (data not shown). *$p < 0.001$ (paired t test). ***B***, MPEP (40 μM) and LY367385 (50 μM) largely prevented DHPG-mediated changes in the sADP in both cell types. Inclusion of ZD7288 (10 μM) in the recording pipette produced a larger sADP than control conditions. Data are from bursts of 5 action potentials at 50 Hz. Similar data were obtained for a single or burst of action potentials at 20 Hz (data not shown). *$p < 0.05$ (paired t test). #$p < 0.05$ (independent sample t test, Bonferroni corrected). In 9 of 12 CPn neurons and 4 of 8 COM neurons, the sADP could be measured after DHPG application in the ZD7288 condition. The remaining neurons fired persistently on each trial of the sADP test. ***C***, Including 10 μM ZD7288 in the recording pipette also increased the propensity of both cell types to fire persistently in the presence of DHPG.

0.72 mV, dendrite −62 ± 0.03 mV; COM, soma −66.62 ± 1.00 mV, dendrite −61.69 ± 1.11; data not shown; $p < 0.01$, paired t test). In a subset of experiments, we also compared the functional membrane time constant at the soma versus the dendrite. Interestingly, the functional membrane time constant was faster in the dendrite compared with the soma in both CPn (data not shown; $n = 8$, soma 26.88 ± 1.83 ms, dendrite 9.44 ± 1.62 ms; $p < 0.001$, paired t test) and COM neurons (data not shown; $n = 5$, soma 36.68 ± 2.33 ms, dendrite 17.44 ± 1.17 ms; $p = 0.003$, paired t test). Nevertheless, these data show that the distinct membrane properties of CPn versus COM neurons observed at the soma (Christophe, 2005; Otsuka and Kawaguchi, 2008; Dembrow et al., 2010; Sheets et al., 2011; Avesar and Gulledge, 2012) extend to the dendritic compartment. Furthermore, they suggest that the subthreshold membrane properties of COM neurons are relatively uniform across the extent of the main apical dendrite, whereas CPn neurons appear to have an increasing gradient of I_h.

mGluR modulation of dendritic properties

Changes in dendritic I_h are hypothesized to contribute to the strengthening of mnemonic persistent activity (Wang et al., 2007). We therefore tested whether Group 1 mGluR activation affects I_h-related subthreshold membrane properties in CPn and COM dendrites. Using single-electrode whole-cell recordings from the dendrites (Fig. 7*A*), we measured I_h-related physiological properties in CPn-type ($n = 7$, range 90–425 μm, mean 242.85 ± 43.23 μm from soma) and COM-type ($n = 4$, range 100–180 μm, mean 128.75 ± 17.84 μm from soma) dendrites before and 30 min after a 10 min application of 20 μM DHPG. In CPn-type dendrites, Group 1 mGluR activation resulted in an increase in R_N and a decrease in rebound, resonance, and sag (Fig. 7*B*,*C*; sag not shown; baseline = 1.31 ± 0.10, DHPG = 1.14 ± 0.06; $p < 0.02$, paired t tests). In contrast, in COM-type dendrites, there was no significant change in these same parameters after DHPG application (Fig. 7*B*,*C*; sag not shown; baseline = 1.05 ± 0.01, DHPG = 1.05 ± 0.01; $p > 0.13$, paired t test). Thus, in the dendritic compartment, like the soma, Group 1 mGluR activation produces a change in subthreshold membrane properties of CPn neurons but not COM neurons.

mGluR activation evokes Ca^{2+} waves that can be initiated in the apical dendrite of L5 neurons (Larkum et al., 2003). Because Ca^{2+} waves are associated with the generation of the sADP (Hagenston et al., 2007), we next tested whether the sADP can be evoked locally in the dendritic compartment. As a first test of this hypothesis, we made whole-cell recordings at various distances from the soma in CPn-type ($n = 18$, range 90–425 μm, mean 244 ± 22 μm from soma) and COM-type dendrites ($n = 11$, range 55–305 μm, mean 154 ± 21 μm from soma). The sADP

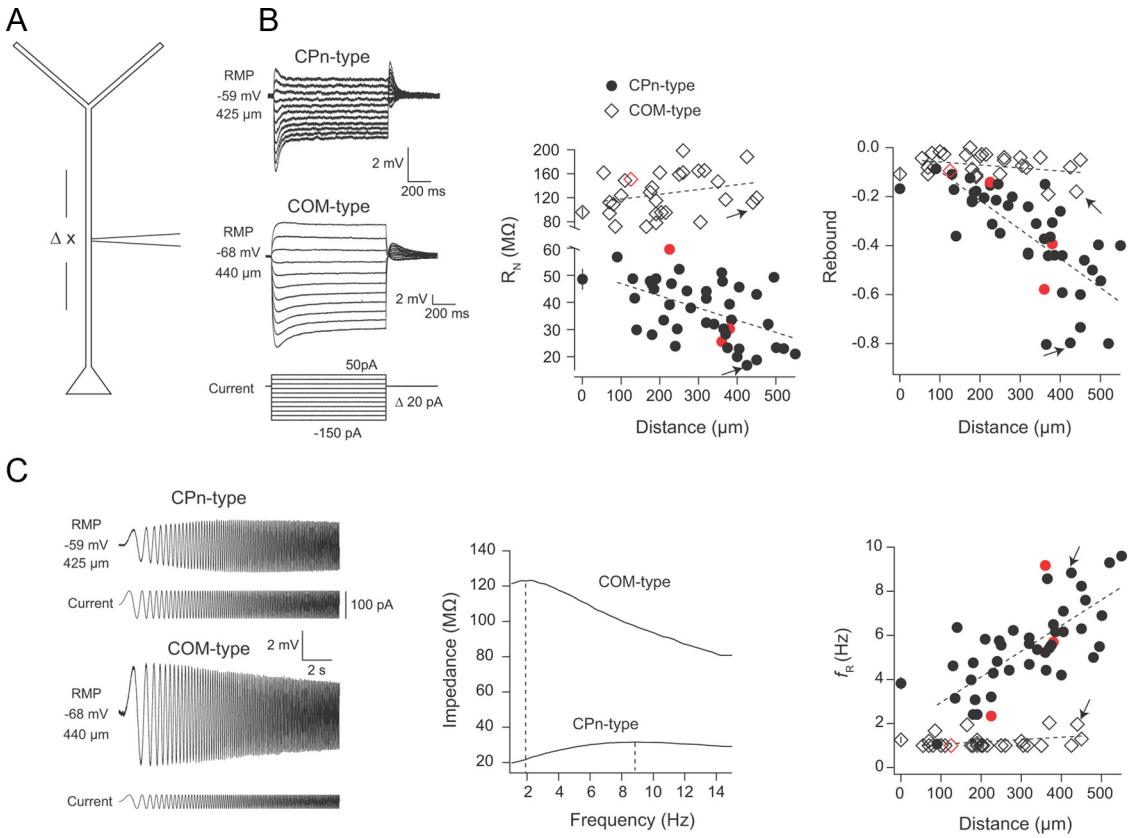

Figure 5. Distance-dependent subthreshold membrane properties of layer 5 dendrites. ***A***, Dendritic recordings at RMP were obtained at various distances from the soma in L5 neurons. We observed two classes of L5 dendrites: those with membrane properties consistent with CPn neurons at the soma (CPn-type) and those with membrane properties consistent with COM neurons at the soma (COM-type). ***B***, In CPn-type dendrites, R_N and rebound slope decreased with distance from the soma (both $p < 0.001$, Pearson's product moment correlation). Conversely, in COM-type dendrites, these measurements were distance independent (both $p = 0.18$, Pearson's product moment correlation). Sample voltage sweeps from which R_N and rebound were calculated are shown at left. ***C***, Resonance increased with distance from the soma in CPn-type dendrites ($p < 0.001$, Pearson's product moment correlation), whereas resonance was ~1 Hz in COM-type dendrites at all distances sampled ($p = 0.10$, Pearson's product moment correlation). Sample voltage sweeps and ZAPs in response to a chirp stimulus for each cell type are shown at left. Average values for R_N, rebound, and resonance from somatic recordings in 12 COM neurons and 13 CPn neurons are also plotted for comparison. Dotted lines represent linear regression fits. R^2 values are reported in the text. Arrows indicate the sample recordings. Red data points denote instances where Lumafluor beads could be clearly identified at the soma. The presence of Alexa-594 in the recording pipette rendered this difficult.

was measured in response to a train of local current injections that evoked 5 spikes at 50 Hz before and 10 min after the application of 20 μM DHPG. Group 1 mGluR activation resulted in an increase in the sADP in both CPn (2.04 ± 0.21 mV after DHPG; $p < 0.001$, paired t test) and COM (4.15 ± 0.54 mV after DHPG; $p < 0.001$, paired t test), neuron types at all measured distances from the soma (Fig. 8; similar results were obtained when considering the integral of the sADP; data not shown). There was a statistically significant decrease in the sADP with distance from the soma in COM-type dendrites ($r^2 = 0.43$, $p = 0.03$), but not CPn-type dendrites ($r^2 = 0.04$, $p = 0.40$). These data establish that Group 1 mGluR activation produces a measurable sADP in the dendritic compartment of both CPn and COM neurons.

To gain insight into the origin of the dendritic sADP, we compared the sADP at the dendrite to the soma using simultaneous somatic and dendritic whole-cell recordings from CPn-type ($n = 9$, range 130–501 μm, mean 266 ± 36 μm between recording sites) and COM-type neurons ($n = 6$, range 85–305 μm, mean 191 ± 29 μm between recording sites; Fig. 9*A*). After a 10 min bath application of DHPG (20 μM), we measured the somatic and dendritic sADP evoked by a burst of 5 spikes at 50 Hz driven by either somatic or dendritic current injection (Fig. 9*B*). The peak amplitude of the sADP at either recording location (soma or dendrite) did not depend on the site of current injection (soma or dendrite) in either cell type (data not shown; all $p > 0.12$; *post hoc* comparisons). Furthermore, for both neuron types, the amplitude of the somatic sADP was slightly larger, or in some cases no different, from the dendritic sADP, regardless of the site of current injection (CPn-type, somatic injection, $p = 0.02$; CPn-type dendritic injection, $p = 0.009$; COM-type, somatic injection, $p < 0.001$; COM-type, dendritic injection, $p = 0.02$; *post hoc* comparison; Fig. 9*C*,*E*).

The small difference in the somatic versus dendritic sADP suggests that the sADP may not simply be passively propagated from the soma to dendrite. To test this hypothesis, we asked whether the difference in the size of the sADP at the dendrite compared with the soma could be explained by passive attenuation. To estimate the passive attenuation of slow events from the soma to dendrite, we injected a current waveform through the somatic electrode to mimic the sADP and measured the response at the soma and dendrite (Fig. 9*D*). The attenuation of the response to the waveform was greater than the difference in the somatic versus dendritic sADP, regardless of the location of current injection (CPn, $p = 0.025$; COM, $p < 0.002$; *post hoc* comparisons; Fig. 9*E*). The location dependence of this phenomenon is shown in Figure 9*F*, where the percentage difference of the

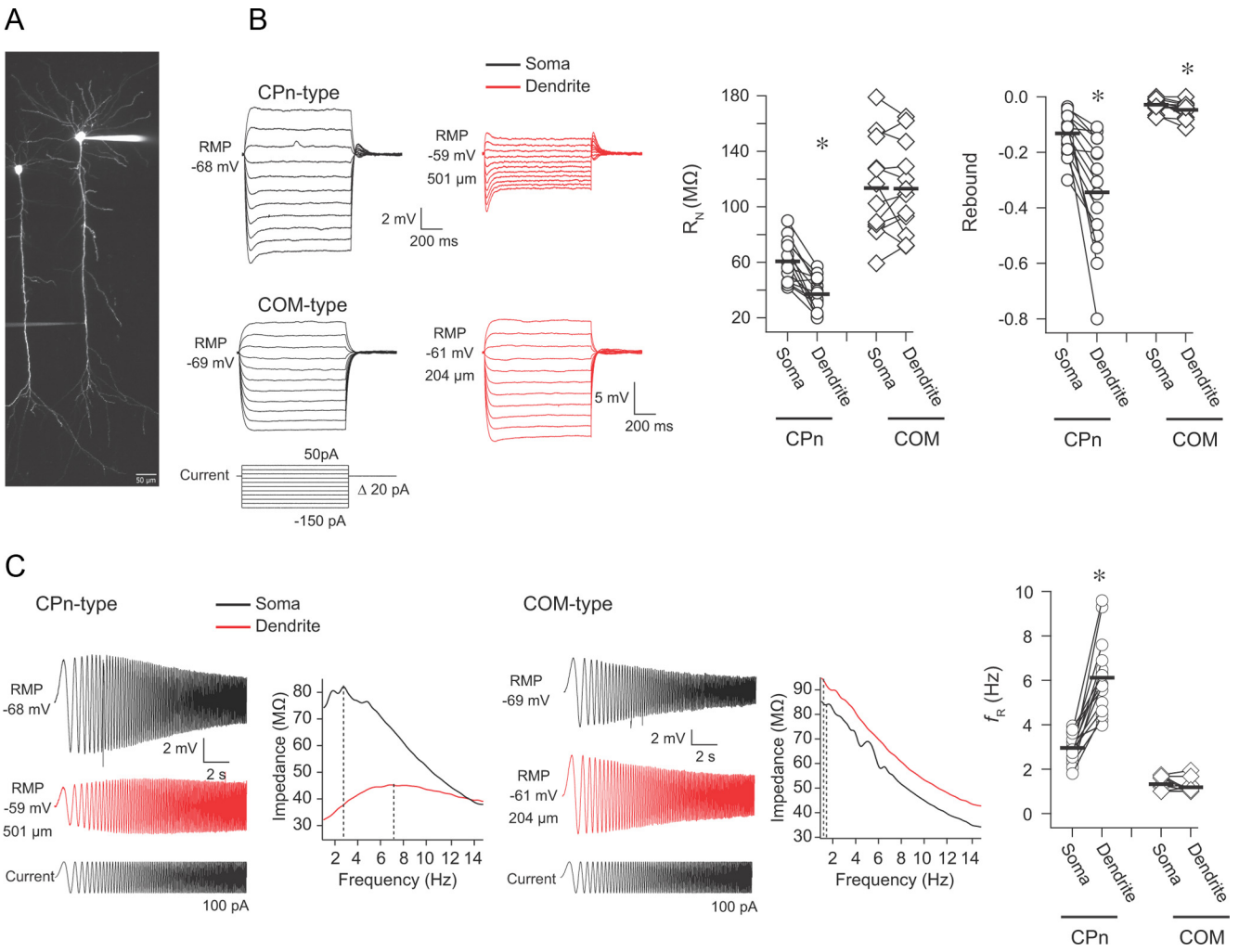

Figure 6. The distinct membrane properties of CPn versus COM neurons at the soma extend to the dendrites. ***A***, Simultaneous somatic and dendritic whole-cell recordings were made from CPn-type and COM-type neurons at RMP. ***B***, Voltage was measured at the soma and dendrite in response to local current injection. Sample voltage responses are shown at left. In CPn neurons, the dendrites had a lower R_N and more rebound compared with the soma. In COM neurons, R_N was high at both the soma and dendrite, and there was a little more rebound at the dendrite compared with the soma. ***C***, In CPn neurons, the dendrite was more resonant than the soma, whereas in COM neurons the soma and dendrite were both nonresonant. Sample voltage responses and ZAPs to a chirp stimulus are shown for each cell type. $^*p < 0.01$ (paired *t* test).

sADP from the passive case is plotted as a function of distance from the soma.

These data provide evidence that mGluR activation produces a measurable sADP at both the soma and dendrite of CPn and COM neurons. Furthermore, it seems that the sADP is not simply passively propagated from the soma to dendrite. This leaves at least two nonmutually exclusive possibilities: (1) the sADP is actively propagated from the soma to the dendrite; and (2) the sADP can be generated locally at multiple sites.

We tested the latter possibility by puffing DHPG (200 μM) in L5, near the soma, or at the L1/L2 border, near the start of the tuft, while recording from the soma or the dendrite (Fig. 10). The puff was followed 3.5 s later by a train of current injections to elicit five spikes at 50 Hz. For somatic recordings, Group 1 mGluR activation in L5 near the soma evoked an sADP in both CPn ($n = 6$; $p = 0.002$; *post hoc* comparison) and COM neurons ($n = 6$; $p = 0.008$; *post hoc* comparison; Fig. 10*A*,*B*). The effect of mGluR activation on the sADP was transient; the size of the sADP was not different from baseline conditions within 1 min of DHPG application in both CPn ($\Delta = 0.18 \pm 0.17$, $p = 0.74$; *post hoc* comparison) and COM neurons ($\Delta = 0.32 \pm 0.24$ $p = 0.64$; *post hoc* comparison; data not shown). In the same experiments, there was no measurable sADP at the soma when DHPG was puffed in L1 (Fig. 10*A*,*B*; CPn, $p = 0.74$; COM, $p = 0.86$; *post hoc* comparisons). These data show that Group 1 mGluR activation near the soma, but not near the apical tuft of L5 neurons, evokes an sADP at the soma.

To test whether local Group 1 mGluR activation can evoke an sADP in the dendrite, we obtained whole-cell recordings from the dendrite of CPn ($n = 7$, range 320–450 μm, mean 375 $\pm$ 16 μm from soma) and COM ($n = 5$, range 200–440 μm, mean 350 $\pm$ 44 μm from soma) neurons (Fig. 10*C*). In this case, puffing DHPG at the L1/L2 border increased the amplitude of the sADP in both CPn ($p = 0.004$; *post hoc* comparison) and COM ($p = 0.02$; *post hoc* comparison) neuron types (Fig. 10*C*,*D*). Similarly, puffing DHPG at the soma, in most cases, produced an sADP at the dendritic recording site in both neuron types (CPn, $p = 0.003$; COM, $p = 0.008$; *post hoc* comparisons; Fig. 10*C*,*D*). The effect of mGluR activation at the dendrite was transient (CPn, $\Delta = 0.54 \pm 0.16$, $p = 0.08$; COM, $\Delta = 0.03 \pm 0.17$, $p = 0.95$; *post hoc* compar-

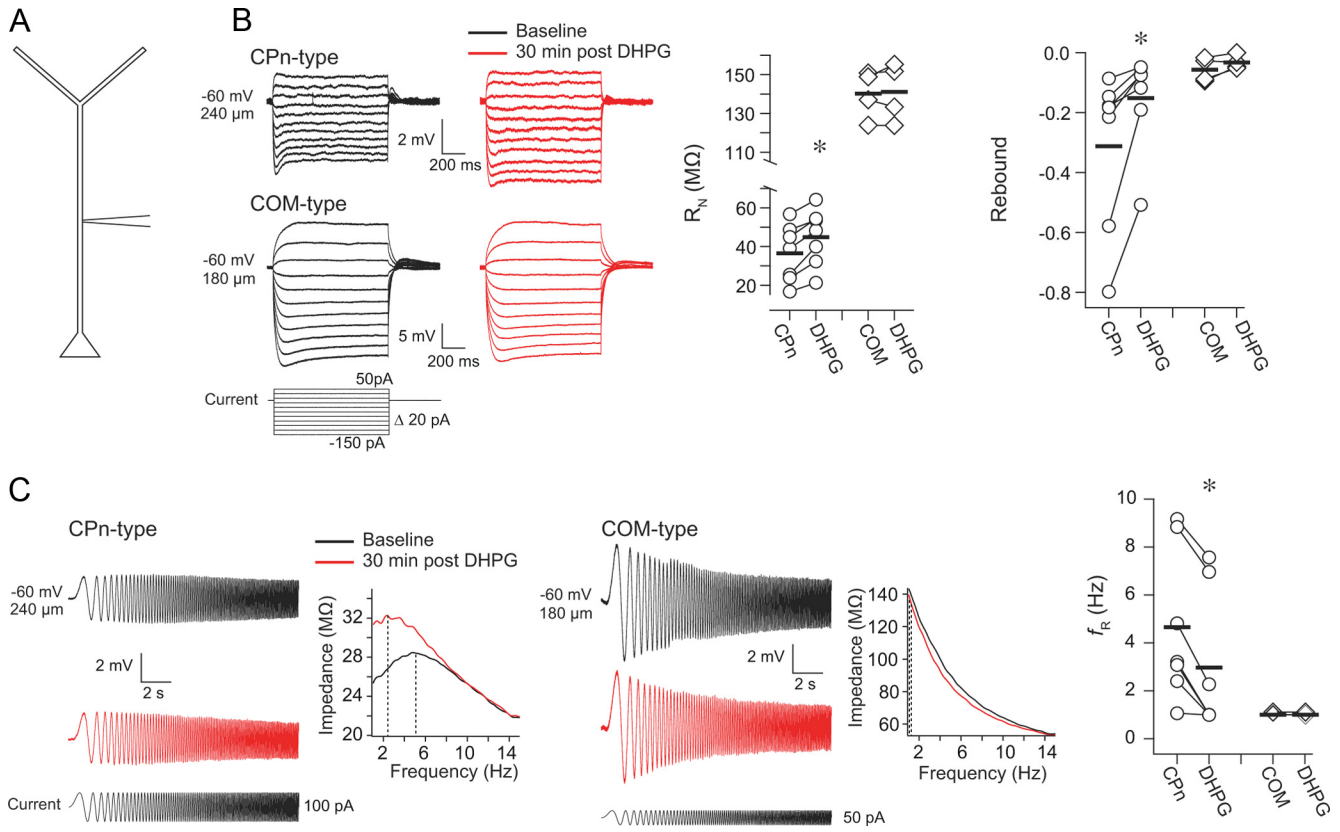

Figure 7. Group 1 mGluR-mediated modulation of subthreshold membrane properties in L5 dendrites. ***A***, I_h-related measurements were made from CPn-type ($n = 7$) and COM-type dendrites ($n = 4$) before and 30 min after a 10 min application of 20 μM DHPG. ***B***, In CPn-type dendrites, DHPG produced an increase in R_N and a decrease in rebound. There were no statistically significant changes in these measures in COM-type dendrites. Sample voltage sweeps from which R_N and rebound were calculated are shown at left. ***C***, Voltage sweeps and their respective ZAPs in response to a chirp stimulus in CPn-type versus COM-type dendrites before and 30 min after a 10 min application of DHPG. DHPG produced a decrease in resonance in CPn neurons, whereas COM neurons remained nonresonant. *$p < 0.02$ (paired test). Measurements were made at −60 mV.

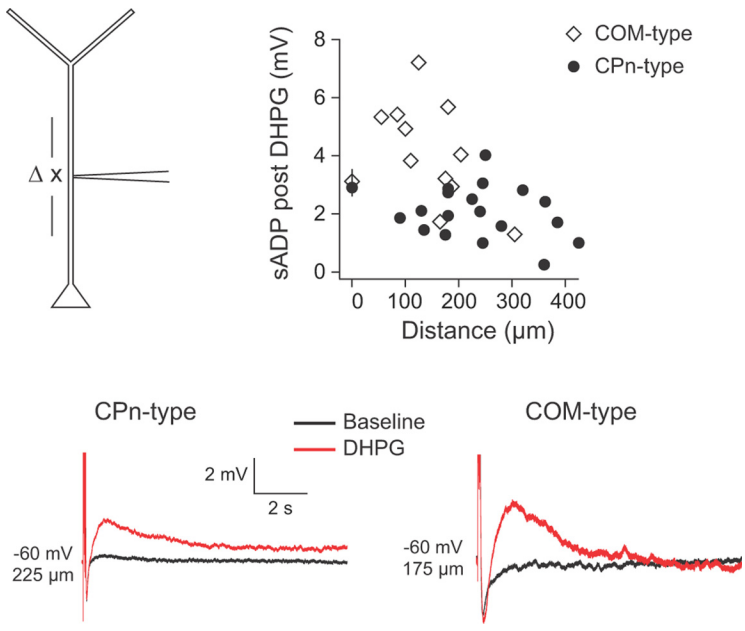

Figure 8. mGluR-mediated sADP in the dendrites of L5 neurons. Whole-cell recordings were obtained from CPn-type ($n = 18$) and COM-type ($n = 11$) neurons at various distances from the soma. A burst of 5 spikes was evoked by brief depolarizing current pulses at the dendritic recording location before and after a 10 min DHPG (20 μM) application. A DHPG-mediated sADP was observed at every recording location in both cell types. Sample sADPs for each cell type are shown below. The average somatic sADP amplitude for 12 CPn neurons and 10 COM neurons is also plotted for reference (same data as Fig. 1).

ison, 1 min post DHPG vs baseline), and there was no statistical difference in the sADP produced by L1/2 versus L5 puffing (CPn, $p = 0.80$; COM, $p = 0.26$; *post hoc* comparisons). These data demonstrate that the activation of Group 1 mGluRs in the dendrite produce a local dendritic sADP.

Discussion

We have provided evidence that there is a dendritic contribution to two putative mechanisms of persistent activity in L5 mPFC pyramidal neurons. Group 1 mGluR activation produced long-term changes in the subthreshold membrane properties of CPn, but not COM neurons. These changes are consistent with a decrease in I_h and are observed at both the soma and apical dendrite. Additionally, mGluR activation transiently increases the amplitude of the sADP in CPn and COM neurons. We observed an sADP along the extent of the main apical dendrite, from the soma to the start of the tuft. Although the dendritic sADP was slightly smaller than the somatic sADP, this difference was less than the difference ob-

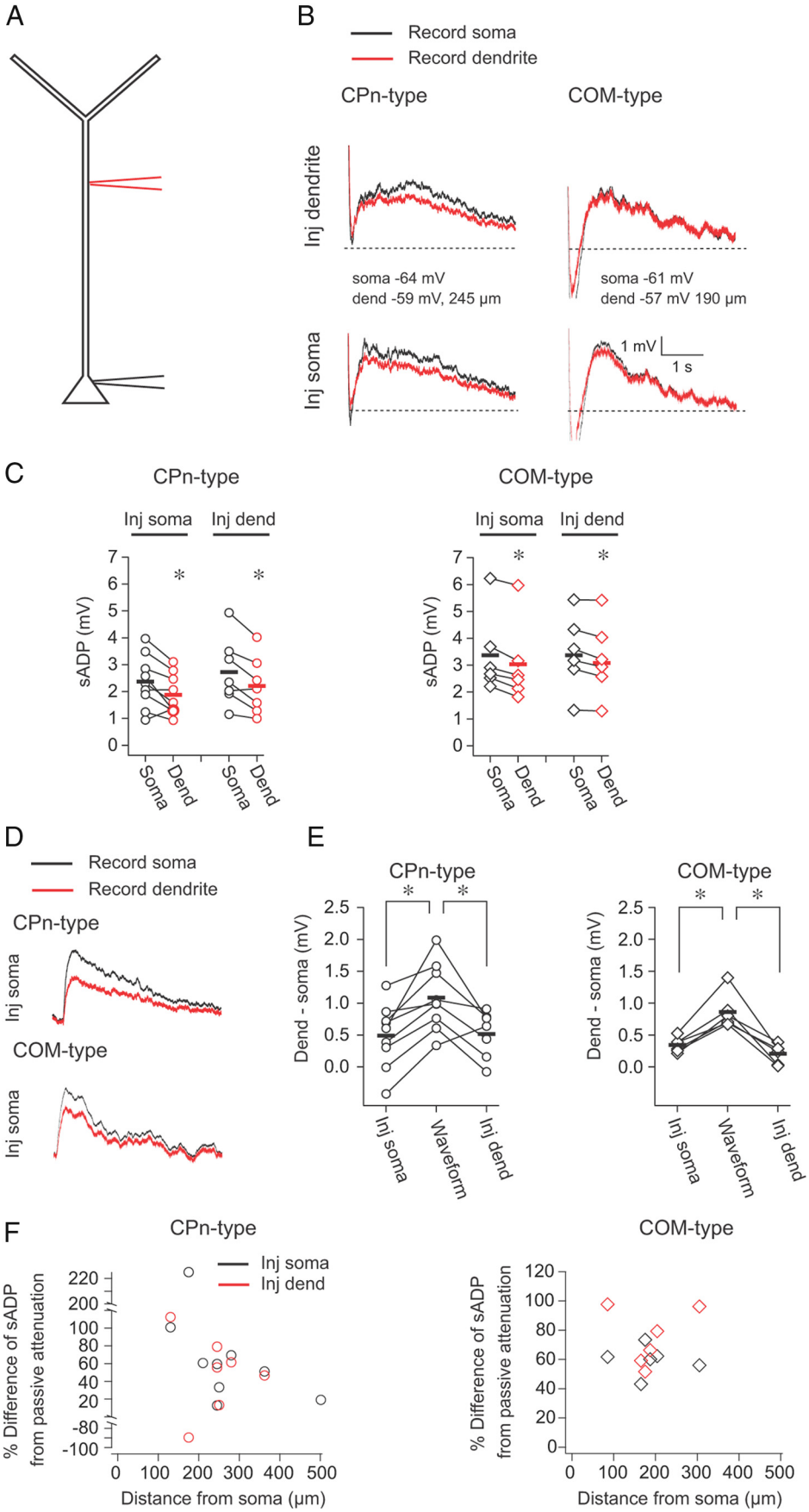

Figure 9. The sADP is not simply passively propagated from the soma to the dendrite. ***A***, Simultaneous whole-cell dendritic and somatic recordings were obtained from CPn-type and COM-type neurons. ***B***, In the presence of 20 μM DHPG, current was injected either at the soma or dendrite to evoke 5 spikes at 50 Hz. The sADP was measured simultaneously at the (*Figure legend continues.*)

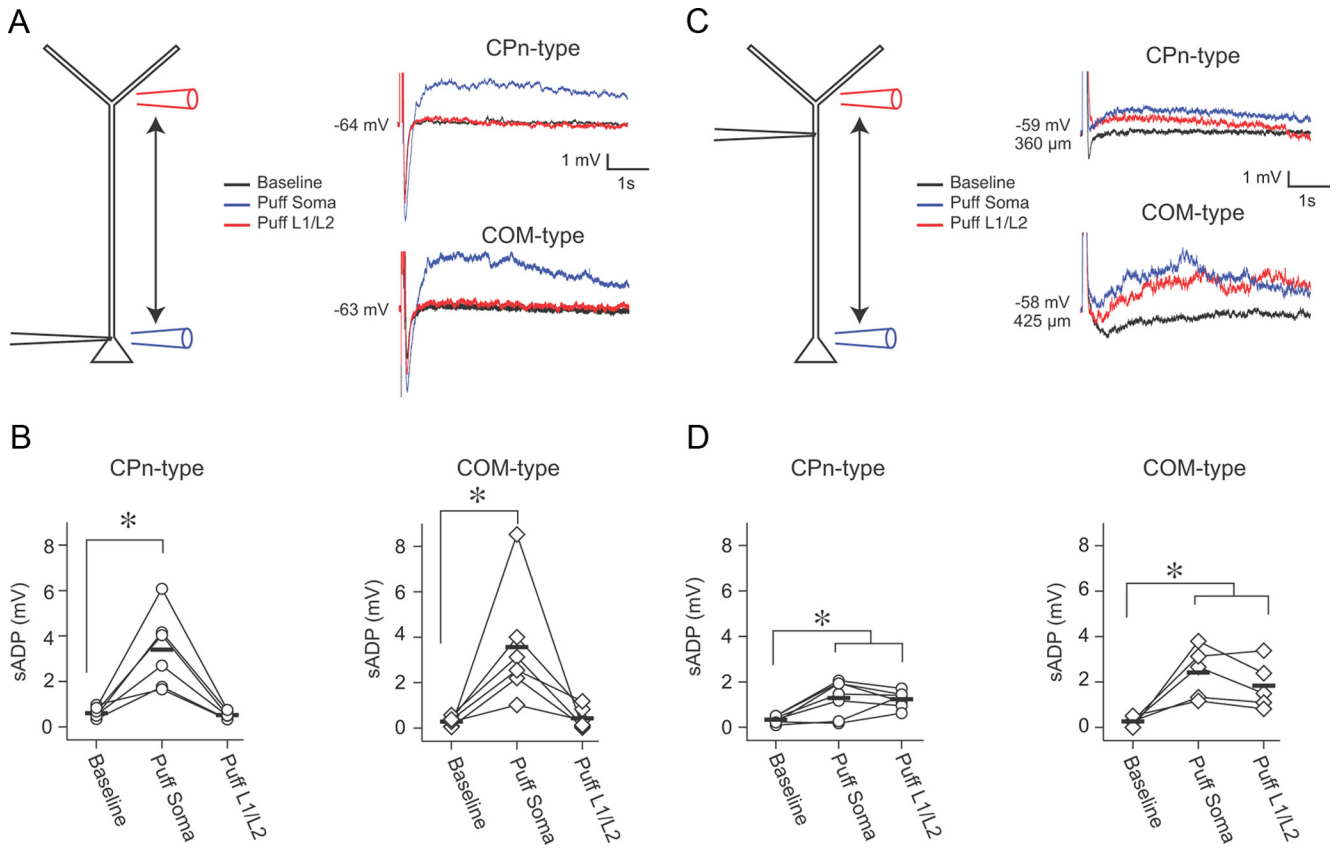

Figure 10. Local dendritic mGluR-mediated sADPs in L5 neurons. ***A***, Whole-cell recordings were obtained from the soma of CPn and COM neurons. DHPG was puffed either in L5 near the soma or at the border of L1/L2, near the start of the tuft. Modulation of the sADP was probed 3.5 s later by evoking a burst of 5 action potentials. ***B***, mGluR activation near the soma modulated the size of the sADP in both neuron types. Puffing in L1 did not produce any detectable change in the sADP at the soma in either cell type (CPn, $p < 0.001$; COM, $p = 0.001$; RM-ANOVA). *$p < 0.008$ (*post hoc* comparisons). ***C***, Same experimental design as *A*, except that recordings were obtained from the dendrite. ***D***, mGluR activation near the soma or in L1 modulated the sADP as observed at the dendrite in both neuron types (CPn, $p < 0.001$; COM, $p < 0.001$; RM-ANOVA). *$p < 0.025$ (*post hoc* comparisons).

served for signals passively propagated from the soma. Thus, the sADP at the dendrite does not solely reflect passive attenuation of the sADP from the soma. Perhaps most importantly, local activation of mGluRs bestow the soma or dendrite the ability to generate an sADP.

Projection-specific dendritic membrane properties

L5 pyramidal neurons have distinct membrane properties, intracortical connectivity, and morphology depending on their long-range projection target (Christophe, 2005; Molnár and Cheung, 2006; Morishima, 2006; Hattox and Nelson, 2007; Otsuka and Kawaguchi, 2008; Brown and Hestrin, 2009; Anderson et al., 2010; Dembrow et al., 2010; Sheets et al., 2011; Avesar and Gulledge, 2012). Based on these observations, it has been proposed that L5 pyramidal neurons can be segregated into two classes: those projecting solely within the telencephalon (e.g., COM neurons; intratelencephalic [IT]) and those with projections outside of the telencephalon (Reiner, 2010; Shepherd, 2013) (e.g., CPn neurons; pyramidal tract [PT]). We have extended these findings to show that the two projection classes have distinct dendritic membrane properties. Specifically, the different subthreshold membrane properties of CPn/PT versus COM/IT neurons observed at the soma (Christophe, 2005; Molnár and Cheung, 2006; Otsuka and Kawaguchi, 2008; Dembrow et al., 2010; Sheets et al., 2011; Avesar and Gulledge, 2012; Gee et al., 2012) extend to the dendritic compartment. CPn neurons display membrane resonance at the dendrite and soma. In contrast, COM neurons display little or no resonance at the soma and dendrite. Furthermore, the subthreshold membrane properties of CPn neurons are consistent with an increasing gradient of I_h with distance from the soma. This is consistent with evidence that HCN1 subunit expression and I_h increase with distance from the soma in some L5 neurons (Williams and Stuart, 2000; Berger et al., 2001; Lörincz et al., 2002; Atkinson and Williams, 2009; Breton and Stuart, 2009). In contrast, COM neurons have I_h-dependent membrane parameters that are relatively uniform across the extent of the apical dendrite. How these distinct membrane properties influence synaptic integration and the transfer of dynamic signals to the soma remains an important question for future studies.

What accounts for differences in subthreshold membrane properties in CPn/PT versus COM/IT neurons? One possibility is

←

(*Figure legend continued.*) soma and dendrite at RMP. ***C***, The amplitude of the sADP was larger at the soma compared with the dendrite regardless of the location of current injection (CPn, $p = 0.01$; COM, $p = 0.01$, RM-ANOVA). *$p < 0.02$ (*post hoc* comparisons). ***D***, A current waveform was injected through the somatic electrode to measure the passive attenuation of slow sADP-like events. ***E***, The attenuation of the response to the waveform was greater than the difference in the amplitude of the sADP at the soma compared with the dendrite (CPn, $p = 0.003$; COM, $p = 0.002$, RM-ANOVA). *$p < 0.025$ (*post hoc* comparisons). ***F***, The percentage difference of the attenuation of the sADP relative to the attenuation of the response to the waveform is plotted as a function of distance between the recording locations for both cell types.

that CPn/PT neurons express HCN channels whereas COM/PT neurons do not. However, the HCN channel blocker ZD7288 produces changes in the subthreshold properties of both neuron types at the soma (Dembrow et al., 2010) and dendrite (our unpublished observations). Thus, both neuron types appear to express I_h. An alternative explanation is that differences in HCN channel composition/expression contribute to the distinct subthreshold membrane properties of CPn versus COM neurons. This is conceivable as the subunit composition of HCN channels (i.e., HCN1 vs HCN2) greatly influences the kinetics of I_h (Santoro et al., 2000; Chen et al., 2001). Furthermore, the expression of HCN1 mRNA is greater in PT compared with IT neurons (Sheets et al., 2011; but see Christophe et al., 2005). Finally, differences in the gradient of HCN channels along the dendrite may contribute to the different membrane properties observed in CPn versus COM neurons. Additional experiments are required to determine how differences in the expression of I_h and other currents contribute to the distinct subthreshold membrane properties of CPn/PT versus COM/IT neurons.

Projection-specific modulation of membrane properties in L5 neurons

In addition to possessing different membrane properties, CPn/PT and COM/IT neurons respond distinctly to various neurotransmitter systems (reviewed in Shepherd, 2013). The activation of α2a noradrenergic receptors, mAChRs, and D2-dopamine receptors appears to have a larger effect on CPn/PT compared with COM/IT neurons (Gee et al., 2003; Dembrow et al., 2010; Sheets et al., 2011). In contrast, D1-dopamine receptor activation appears to only affect COM/IT neurons, whereas 5-HT receptor activation has opposite effects on the two projection classes (Avesar and Gulledge, 2012; Seong and Carter, 2012). Here, we show that mGluR activation has similar effects on the sADP in COM versus CPn neurons, yet only CPn neurons displayed long-term changes in subthreshold membrane properties. Thus, the same neurotransmitter can evoke similar or divergent effects, depending on the membrane property in question, in CPn versus COM neurons.

Our data are also, to our knowledge, the first demonstration that I_h decreases in the dendrites of prefrontal neurons after the activation of a neurotransmitter system implicated in working memory (Homayoun et al., 2004; Homayoun and Moghaddam, 2010). The modulation of I_h is thought to be essential for the generation of persistent activity (Wang et al., 2007). Somatic whole-cell recordings have shown that there is a decrease in I_h after the activation of neurotransmitter systems important for persistent activity *in vivo* (Carr et al., 2007; Dembrow et al., 2010). Because I_h is enriched in the dendrite (Magee, 1998; Williams and Stuart, 2000; Atkinson and Williams, 2009; Breton and Stuart, 2009), these changes are proposed to occur in the dendritic compartment. Consistent with this, we show that I_h-related membrane properties, including resonance, which reflects local I_h (Narayanan and Johnston, 2007, 2008), change in the main apical dendrite of CPn neurons after mGluR activation.

Dendritic mGluR activation generates Ca^{2+} waves along the extent of the main apical dendrite of cortical pyramidal neurons (Larkum et al., 2003). The amplitude of the sADP at the soma depends on whether the Ca^{2+} wave invades the soma (Hagenston et al., 2007). We expand these findings to show that there is an sADP in the dendrite of CPn and COM neurons upon mGluR activation. This dendritic sADP is not simply passively propagated from the soma and can be evoked via local activation of mGluRs. Given that we failed to see an sADP at the soma after mGluR activation in the dendrite, the dendritic sADP may attenuate greatly as it spreads to the soma. Alternatively, it is possible that action potentials fail to propagate to the dendrite sufficiently to generate an sADP. Whether Ca^{2+} waves, backpropagating action potentials, and/or local regenerative events contribute to the generation and propagation of dendritically initiated sADPs remain intriguing questions.

Functional relevance

Although it remains to be seen whether synaptically evoked glutamate produces similar effects, there are several possible functional consequences of the mGluR-mediated changes we have described. Persistent activity has been proposed to involve both cell autonomous and network-related mechanisms. Downregulation of I_h is implicated in strengthening networks of reciprocally connected neurons (Wang et al., 2007), whereas the sADP has been proposed to contribute to self-sustained single-cell persistent activity (Schwindt et al., 1988; Haj-Dahmane and Andrade, 1998; Hasselmo and Stern, 2006; Sidiropoulou et al., 2009). Our data suggest that mGluR activation can engage both types of mechanisms; therefore, persistent activity may involve cell autonomous and network mechanisms. Because subthreshold changes were restricted to CPn neurons, one implication of our work is that mGluR activation is involved in strengthening CPn/PT networks in particular. This possibility is especially intriguing in light of evidence that CPn/PT pairs display a higher rate of reciprocity than COM/IT pairs (Morishima et al., 2011). Our results also suggest a novel role for the downregulation of I_h in the generation of persistent activity. Blocking I_h increased the sADP and the occurrence of self-sustaining, single-cell persistent activity. This suggests that, in addition to enhancing integration, downregulating I_h may increase the likelihood of persistent activity through its effect on the sADP. This hypothesis may provide insight into how multiple neurotransmitter systems converge to modulate persistent activity. In this framework, mGluR (or mAChR) activation is responsible for generating an sADP. Coincident α2a noradrenergic receptor activation would increase the probability of generating persistent activity through its indirect effects on the sADP via modulation of I_h.

Currently, the functional consequences of a sustained dendritic depolarization are purely speculative. At the soma, the sADP can convert subthreshold events into suprathreshold spiking (Sidiropoulou et al., 2009). Synaptic inputs arriving coincidentally with the dendritic sADP may be similarly enhanced and contribute to spiking at the soma. Assuming that the sADP at the dendrite, like at the soma (Greene et al., 1994), increases in amplitude with depolarization, synaptic inputs arriving during the sADP could further reinforce this phenomenon. In this way, the sADP may represent an interval in which the neuron is especially sensitive to inputs arriving in the main apical dendrite. The ability of inputs arriving at different layers to enhance the sensitivity of the dendrite represents an intriguing, yet untested, possibility.

References

Anderson CT, Sheets PL, Kiritani T, Shepherd GM (2010) Sublayer-specific microcircuits of corticospinal and corticostriatal neurons in motor cortex. Nat Neurosci 13:739–744. CrossRef Medline

Anwyl R (1999) Metabotropic glutamate receptors: electrophysiological properties and role in plasticity. Brain Res Brain Res Rev 29:83–120. CrossRef Medline

Atkinson SE, Williams SR (2009) Postnatal development of dendritic synaptic integration in rat neocortical pyramidal neurons. J Neurophysiol 102:735–751. CrossRef Medline

Avesar D, Gulledge AT (2012) Selective serotonergic excitation of callosal projection neurons. Front Neural Circuits 6:12. CrossRef Medline

Berger T, Larkum ME, Lüscher HR (2001) High I(h) channel density in the distal apical dendrite of layer V pyramidal cells increases bidirectional attenuation of EPSPs. J Neurophysiol 85:855–868. Medline

Brager DH, Johnston D (2007) Plasticity of intrinsic excitability during long-term depression is mediated through mGluR-dependent changes in Ih in hippocampal CA1 pyramidal neurons. J Neurosci 27:13926–13937. CrossRef Medline

Bremner JD, Narayan M, Staib LH, Southwick SM, McGlashan T, Charney DS (1999) Neural correlates of memories of childhood sexual abuse in women with and without posttraumatic stress disorder. Am J Psychiatry 156:1787–1795. Medline

Breton JD, Stuart GJ (2009) Loss of sensory input increases the intrinsic excitability of layer 5 pyramidal neurons in rat barrel cortex. J Physiol 587:5107–5119. CrossRef Medline

Brown SP, Hestrin S (2009) Intracortical circuits of pyramidal neurons reflect their long-range axonal targets. Nature 457:1133–1136. CrossRef Medline

Carr DB, Andrews GD, Glen WB, Lavin A (2007) alpha2-Noradrenergic receptors activation enhances excitability and synaptic integration in rat prefrontal cortex pyramidal neurons via inhibition of HCN currents. J Physiol 584:437–450. CrossRef Medline

Chen S, Wang J, Siegelbaum SA (2001) Properties of hyperpolarization-activated pacemaker current defined by coassembly of HCN1 and HCN2 subunits and basal modulation by cyclic nucleotide. J Gen Physiol 117:491–504. CrossRef Medline

Christophe E, Doerflinger N, Lavery DJ, Molnár Z, Charpak S, Audinat E (2005) Two populations of layer V pyramidal cells of the mouse neocortex: development and sensitivity to anesthetics. J Neurophysiol 94:3357–3367. CrossRef Medline

Courchesne E, Pierce K (2005) Why the frontal cortex in autism might be talking only to itself: local over-connectivity but long-distance disconnection. Curr Opin Neurobiol 15:225–230. CrossRef Medline

Dembrow NC, Chitwood RA, Johnston D (2010) Projection-specific neuromodulation of medial prefrontal cortex neurons. J Neurosci 30:16922–16937. CrossRef Medline

Egan MF, Weinberger DR (1997) Neurobiology of schizophrenia. Curr Opin Neurobiol 7:701–707. CrossRef Medline

Egorov AV, Hamam BN, Fransén E, Hasselmo ME, Alonso AA (2002) Graded persistent activity in entorhinal cortex neurons. Nature 420:173–178. CrossRef Medline

Fineberg NA, Potenza MN, Chamberlain SR, Berlin HA, Menzies L, Bechara A, Sahakian BJ, Robbins TW, Bullmore ET, Hollander E (2009) Probing compulsive and impulsive behaviors, from animal models to endophenotypes: a narrative. Rev Neuropsychopharmacol 35:591–604. CrossRef Medline

Funahashi S, Bruce CJ, Goldman-Rakic PS (1989) Mnemonic coding of visual space in the monkey's dorsolateral prefrontal cortex. J Neurophysiol 61:331–349. Medline

Fuster JM (2001) The prefrontal cortex—an update: time is of the essence. Neuron 30:319–333. CrossRef Medline

Gee CE, Benquet P, Gerber U (2003) Group I metabotropic glutamate receptors activate a calcium-sensitive transient receptor potential-like conductance in rat hippocampus. J Physiol 546:655–664. CrossRef Medline

Gee S, Ellwood I, Patel T, Luongo F, Deisseroth K, Sohal VS (2012) Synaptic activity unmasks dopamine D2 receptor modulation of a specific class of layer V pyramidal neurons in prefrontal cortex. J Neurosci 32:4959–4971. CrossRef Medline

Goldman-Rakic PS (1995) Cellular basis of working memory. Neuron 14:477–485. CrossRef Medline

Goldstein RZ, Volkow ND (2011) Dysfunction of the prefrontal cortex in addiction: neuroimaging findings and clinical implications. Nat Rev Neurosci 12:652–669. CrossRef Medline

Greene CC, Schwindt PC, Crill WE (1994) Properties and ionic mechanisms of a metabotropic glutamate receptor-mediated slow afterdepolarization in neocortical neurons. J Neurophysiol 72:693–704. Medline

Hagenston AM, Fitzpatrick JS, Yeckel MF (2008) MGluR-mediated calcium waves that invade the soma regulate firing in layer V medial prefrontal cortical pyramidal neurons. Cereb Cortex 18:407–423. CrossRef Medline

Haj-Dahmane S, Andrade R (1996) Muscarinic activation of a voltage-dependent cation nonselective current in rat association cortex. J Neurosci 16:3848–3861. Medline

Haj-Dahmane S, Andrade R (1998) Ionic mechanism of the slow afterdepolarization induced by muscarinic receptor activation in rat prefrontal cortex. J Neurophysiol 80:1197–1210. Medline

Hasselmo ME, Stern CE (2006) Mechanisms underlying working memory for novel information. Trends Cogn Sci (Regul Ed) 10:487–493. CrossRef Medline

Hattox AM, Nelson SB (2007) Layer V neurons in mouse cortex projecting to different targets have distinct physiological properties. J Neurophysiol 98:3330–3340. CrossRef Medline

Homayoun H, Moghaddam B (2010) Group 5 metabotropic glutamate receptors: role in modulating cortical activity and relevance to cognition. Eur J Pharmacol 639:33–39. CrossRef Medline

Homayoun H, Stefani MR, Adams BW, Tamagan GD, Moghaddam B (2004) Functional interaction between NMDA and mGlu5 receptors: effects on working memory, instrumental learning, motor behaviors, and dopamine release. Neuropsychopharmacology 29:1259–1269. CrossRef Medline

Hu H, Vervaeke K, Storm JF (2002) Two forms of electrical resonance at θ frequencies, generated by M-current, h-current and persistent Na^+ current in rat hippocampal pyramidal cells. J Physiol 545:783–805. CrossRef Medline

Hutcheon B, Yarom Y (2000) Resonance, oscillation and the intrinsic frequency preferences of neurons. Trends Neurosci 23:216–222. CrossRef Medline

Hutcheon B, Miura RM, Puil E (1996) Subthreshold membrane resonance in neocortical neurons. J Neurophysiol 76:683–697. Medline

Jung MW, Qin Y, McNaughton BL, Barnes CA (1998) Firing characteristics of deep layer neurons in prefrontal cortex in rats performing spatial working memory tasks. Cereb Cortex 8:437–450. CrossRef Medline

Krause M, Offermanns S, Stocker M, Pedarzani P (2002) Functional specificity of G α q and G α 11 in the cholinergic and glutamatergic modulation of potassium currents and excitability in hippocampal neurons. J Neurosci 22:666–673. Medline

Larkum ME, Watanabe S, Nakamura T, Lasser-Ross N, Ross WN (2003) Synaptically activated Ca^{2+} waves in layer 2/3 and layer 5 rat neocortical pyramidal neurons. J Physiol 549:471–488. CrossRef Medline

Lörincz A, Notomi T, Tamás G, Shigemoto R, Nusser Z (2002) Polarized and compartment-dependent distribution of HCN1 in pyramidal cell dendrites. Nat Neurosci 5:1185–1193. CrossRef Medline

Magee JC (1998) Dendritic hyperpolarization-activated currents modify the integrative properties of hippocampal CA1 pyramidal neurons. J Neurosci 18:7613–7624. Medline

Mannaioni G, Marino MJ, Valenti O, Traynelis SF, Conn PJ (2001) Metabotropic glutamate receptors 1 and 5 differentially regulate CA1 pyramidal cell function. J Neurosci 21:5925–5934. Medline

Miller EK (2000) The prefrontal cortex and cognitive control. Nat Rev Neurosci 1:59–65. CrossRef Medline

Molnár Z, Cheung AF (2006) Towards the classification of subpopulations of layer V pyramidal projection neurons. Neurosci Res 55:105–115. CrossRef Medline

Morishima M, Kawaguchi Y (2006) Recurrent connection patterns of corticostriatal pyramidal cells in frontal cortex. J Neurosci 26:4394–4405. CrossRef Medline

Morishima M, Morita K, Kubota Y, Kawaguchi Y (2011) Highly differentiated projection-specific cortical subnetworks. J Neurosci 31:10380–10391. CrossRef Medline

Narayanan R, Johnston D (2007) Long-term potentiation in rat hippocampal neurons is accompanied by spatially widespread changes in intrinsic oscillatory dynamics and excitability. Neuron 56:1061–1075. CrossRef Medline

Narayanan R, Johnston D (2008) The h channel mediates location dependence and plasticity of intrinsic phase response in rat hippocampal neurons. J Neurosci 28:5846–5860. CrossRef Medline

Nolan MF, Malleret G, Dudman JT, Buhl DL, Santoro B, Gibbs E, Vronskaya S, Buzsáki G, Siegelbaum SA, Kandel ER, Morozov A (2004) A behavioral role for dendritic integration: HCN1 channels constrain spatial memory and plasticity at inputs to distal dendrites of CA1 pyramidal neurons. Cell 119:719–732. CrossRef Medline

Otsuka T, Kawaguchi Y (2008) Firing-pattern-dependent specificity of cortical excitatory feed-forward subnetworks. J Neurosci 28:11186–11195. CrossRef Medline

Pasupathy A, Miller EK (2005) Different time courses of learning-related

activity in the prefrontal cortex and striatum. Nature 433:873–876. CrossRef Medline

Poolos NP, Migliore M, Johnston D (2002) Pharmacological upregulation of h-channels reduces the excitability of pyramidal neuron dendrites. Nat Neurosci 5:767–774. CrossRef Medline

Reiner A, Hart NM, Lei W, Deng Y (2010) Corticostriatal projection neurons: dichotomous types and dichotomous functions. Front Neuroanat 4:142. CrossRef Medline

Rich EL, Shapiro M (2009) Rat prefrontal cortical neurons selectively code strategy switches. J Neurosci 29:7208–7219. CrossRef Medline

Rich EL, Shapiro ML (2007) Prelimbic/infralimbic inactivation impairs memory for multiple task switches, but not flexible selection of familiar tasks. J Neurosci 27:4747–4755. CrossRef Medline

Robinson RB, Siegelbaum SA (2003) Hyperpolarization-activated cation currents: from molecules to physiological function. Annu Rev Physiol 65:453–480. CrossRef Medline

Santoro B, Chen S, Luthi A, Pavlidis P, Shumyatsky GP, Tibbs GR, Siegelbaum SA (2000) Molecular and functional heterogeneity of hyperpolarization-activated pacemaker channels in the mouse CNS. J Neurosci 20:5264–5275. Medline

Schwindt PC, Spain WJ, Foehring RC, Chubb MC, Crill WE (1988) Slow conductances in neurons from cat sensorimotor cortex in vitro and their role in slow excitability changes. J Neurophysiol 59:450–467. Medline

Seong HJ, Carter AG (2012) D1 receptor modulation of action potential firing in a subpopulation of layer 5 pyramidal neurons in the prefrontal cortex. J Neurosci 32:10516–10521. CrossRef Medline

Sheets PL, Suter BA, Kiritani T, Chan CS, Surmeier DJ, Shepherd GM (2011) Corticospinal-specific HCN expression in mouse motor cortex: Ih-dependent synaptic integration as a candidate microcircuit mechanism involved in motor control. J Neurophysiol 106:2216–2231. CrossRef Medline

Shepherd GM (2013) Corticostriatal connectivity and its role in disease. Nat Rev Neurosci 14:278–291. CrossRef Medline

Sidiropoulou K, Lu FM, Fowler MA, Xiao R, Phillips C, Ozkan ED, Zhu MX, White FJ, Cooper DC (2009) Dopamine modulates an mGluR5-mediated depolarization underlying prefrontal persistent activity. Nat Neurosci 12:190–199. CrossRef Medline

Sourdet V, Russier M, Daoudal G, Ankri N, Debanne D (2003) Long-term enhancement of neuronal excitability and temporal fidelity mediated by metabotropic glutamate receptor subtype 5. J Neurosci 23:10238–10248. Medline

Wang M, Ramos BP, Paspalas CD, Shu Y, Simen A, Duque A, Vijayraghavan S, Brennan A, Dudley A, Nou E, Mazer JA, McCormick DA, Arnsten AF (2007) α2A-adrenoceptors strengthen working memory networks by inhibiting cAMP-HCN channel signaling in prefrontal cortex. Cell 129:397–410. CrossRef Medline

Williams SR, Stuart GJ (2000) Site independence of EPSP time course is mediated by dendritic I(h) in neocortical pyramidal neurons. J Neurophysiol 83:3177–3182. Medline

Yoshida M, Fransén E, Hasselmo ME (2008) mGluR-dependent persistent firing in entorhinal cortex layer III neurons. Eur J Neurosci 28:1116–1126. CrossRef Medline

Young SR, Chuang SC, Wong RK (2004) Modulation of afterpotentials and firing pattern in guinea pig CA3 neurones by group I metabotropic glutamate receptors. J Physiol 554:371–385. CrossRef Medline